

# Experimental Study on the Viscoplastic Response and Buckling of Local Sharp-notched SUS304 Stainless Steel Tubes under Cyclic Bending

Kuo-Long Lee<sup>1</sup>, Yu-An Chen<sup>2</sup>, Wen-Fung Pan<sup>3</sup>

1(Department of Innovative Design and Entrepreneurship Management, Far East University, Tainan, Taiwan)

2 (Department of engineering Science, National Cheng Kung University, Tainan, Taiwan)

3 (Department of engineering Science, National Cheng Kung University, Tainan, Taiwan)

## Abstract:

In this paper, the experiment for inspecting the response and buckling of local sharp-notched SUS304 stainless steel tubes with different notch depths subjected to cyclic bending at different curvature rates is presented. Tubes with notch depths varying from very shallow (0.2 mm) to approximately 2/3 times the tube wall thickness (1.0 mm) were considered. Three different curvature rates, 0.0035, 0.035 and 0.35  $m^{-1}s^{-1}$ , were used in the test for highlighting the viscoplastic response and buckling. The experimental moment-curvature relationships showed a nearly closed and steady hysteresis loop after a few bending cycles. Higher curvature rates led to larger cyclic steady loop. The experimental ovalization-curvature relationships showed an increase in asymmetry and ratcheting with an increase in the number of bending cycles. Deep notch depths and higher curvature rates caused larger ovalization. The experimental controlled curvature-number of bending cycles required to produce buckling relationships demonstrated that for a fixed controlled curvature and notch depth, a larger curvature rate led to a lower number of bending cycles required to produce buckling. In addition, for a fixed controlled curvature and notch depth curvature rate, a larger notch depth caused a lower number of bending cycles required to produce buckling.

**Keywords** — Local sharp notch, SUS304 stainless steel tubes, cyclic bending, viscoplastic response, viscoplastic buckling, moment, curvature, ovalization, number of bending cycles required to produce buckling.

## I. INTRODUCTION

From 1985, Kyriakides' team began a series of experimental and theoretical studies on tubes subjected to monotonic and cyclic bending, as well as with and without external or internal pressure. Shaw and Kyriakides [1] investigated the elastic-plastic response of thin-walled tubes under cyclic bending. They showed a gradual increase in the tube's ovalization during reverse and continuous cyclic bending. Kyriakides and Shaw [2] extended this research to the buckling failure of tubes under cyclic bending. On the basis of this experimental result, an empirical formula was proposed for the relation between the curvature and number of bending cycles required to produce buckling. Corona and Kyriakides [3] experimentally

investigated the weakening and failure of tubes under cyclic bending with external pressure. In their research, the effects of the cyclic bending path with and without external pressure on the ovalization accumulation rate and the timing of buckling were examined. Furthermore, Corona and Kyriakides [4] investigated the failure of tubes subjected to bending with and without external pressure. Asymmetric imperfections and buckling were theoretically evaluated with a previously derived formula. Similarly, Corona et al. [5] discovered that such tubes display plastic anisotropy and described this using Hill's yield criterion. By including the material anisotropy, they evaluated prebuckling, postbuckling, and bifurcation using flow and deformation theories. Limam et al. [6] investigated the failure of locally-dented tubes under pure

bending with internal pressure. Using finite element models, the dent production, tube pressurization, and tube bending for collapse were properly described. Bechle and Kyriakides[7] examined the localization of NiTi tubes subjected to bending. The influence of texture and material asymmetry on the tube structure was studied.

Additionally, other scholars have published a number of related research papers. Yuan and Mirmiran[8] experimentally and theoretically examined the collapse of fiber-reinforced plastic tubes filled with concrete and subjected to bending. Elchalakani et al. [9] tested grade C350 steel tubes with different diameter-to-thickness ratios ( $D_o/t$  ratios) under pure bending. Jiao and Zhao [10] experimentally investigated the plastic slenderness limit of very-high-strength circular steel tubes under bending. Houliara and Karamanos[11] studied the buckling and postbuckling of thin-walled tubes under in-phase bending and internal pressure. Mathon and Liman [12] experimentally studied the collapse of thin-walled tubes subjected to pure bending and internal pressure. Elchalakani and Zhao [13] investigated the response of concrete-filled, cold-formed circular steel tubes subjected to monotonic and cyclic bending with variable amplitudes. Zhi et al. [14] studied the instability and failure of single-layer, cylindrical, reticulated tubes subjected to earthquake motion. Guo et al. [15] discussed the response of thin-walled circular tubes with a hollow subjected to bending. Shariati et al. [16] experimentally studied the SS316L cantilevered cylindrical shells under cyclic bending loads. Elchalakani et al. [17] employed the measured strains in plastic bending tests to determine new ductile slenderness limits for plastic design of CFT structures.

In 1998, Pan's research team started, experimentally and theoretically, to explore different kinds of tubes subjected to monotonic bending or cyclic bending given different loading and geometry conditions. For example, Pan and Her [18] experimentally investigated the viscoplastic failure of SUS304 stainless steel tubes subjected to cyclic bending. To simulate the relationship between the cyclic controlled curvature and the number of bending cycles required to yield buckling, an

empirical form was introduced by them. Lee et al. [19] studied the influence of the  $D_o/t$  ratio on the response and stability of circular tubes subjected to symmetrical cyclic bending. Diverse  $D_o/t$  ratios of SUS304 stainless steel tubes were investigated and an empirical form was suggested for describing the correlation between the cyclic controlled curvature and number of bending cycles required to generate buckling. Lee et al. [20] inspected the cyclic bending stability of 316L stainless steel tubes. The endochronic constitutive model combined with the principle of virtual work was employed to predict the moment-curvature and ovalization-curvature relationships. In addition, Chang and Pan [21] also conducted experiments through which circular tubes' degradation and stability for different outer diameters were investigated. They discovered that the curve of the ovalization vs. number of bending cycles could be separated into initial, secondary and tertiary stages.

Tubes are typically used in harsh environments, which may corrode the surfaces and create notches. Notched tubes should exhibit responses and collapse mechanisms different from their smooth-surfaced counterparts. From 2010, Pan's research group started experimental and theoretical investigations on the response of sharp-notched tubes under cyclic bending. Lee et al. [22] experimentally examined the change in ovalization along with the number of bending cycles for sharp-notched circular tubes subjected to cyclic bending. Three stages (initial, secondary, and tertiary) were clearly observed from the curve of ovalization versus the number of bending cycles. Later, Lee [23] investigated the behavior and failure of sharp-notched SUS304 stainless steel tubes subjected to cyclic bending. Asymmetry, ratcheting, and increasing ovalization-curvature curves were discovered. In addition, Lee et al. [24] experimentally examined the viscoplastic buckling of sharp-notched SUS304 stainless steel circular tubes under cyclic bending, and changes in both the notch depth and curvature rate were examined. Observations of a certain curvature rate revealed that the cyclic-controlled curvature and the number of bending cycles required to yield buckling

relationships at a log-log scale exhibited parallel lines for every notch depth.

Although the viscoplastic response and collapse of sharp-notched SUS304 stainless steel tubes under cyclic bending has been investigated [24], but the type of sharp notch was the circumferential sharp notch as shown in Fig. 1. However, tubes in actual applications are typically used in cruel environments, which may corrode the tube's surface and create a local sharp notch. The response and collapse of local sharp-notched tubes submitted to cyclic bending at different curvature rates should exhibit differing from that of circumferential sharp-notched tubes submitted to cyclic bending at different curvature rates.



Fig. 1 A picture of a circumferential sharp-notched circular tube

In this paper, local sharp-notched SUS304 stainless steel tubes with different notch depths of 0.2, 0.4, 0.6, 0.8 and 1.0 mm under cyclic bending were experimentally studied. In addition, to highlight the viscoplastic phenomenon, three different curvature rates,  $0.0035$ ,  $0.035$  and  $0.35 \text{ m}^{-1} \text{ s}^{-1}$ , were controlled. Note that the experimental data for curvature rate of  $0.035 \text{ m}^{-1} \text{ s}^{-1}$  have been tested by Lee et al. [25]. Other related experimental tests were conducted using a tube-bending machine and curvature-ovalization measurement apparatus. The bending moment, curvature, and ovalization were measured with sensors at the testing facility. The number of bending cycles required to produce buckling was also recorded.

## II. EXPERIMENTS

### A. Bending Device

Fig.2 is a schematic drawing of the bending device. It is designed as a four-point bending

machine, capable of applying bending and reverse bending. The device consists of two rotating sprockets resting on two support beams. Heavy chains run around the sprockets and are connected to two hydraulic cylinders and load cells forming a closed loop. Each tube is tested and fitted with solid rod extension. The contact between the tube and the rollers is free to move along axial direction during bending. The load transfer to the test specimen is in the form of a couple formed by concentrated loads from two of the rollers. Once either the top or bottom cylinder is contracted, the sprockets are rotated, and pure bending of the test specimen is achieved. Reverse bending can be achieved by reversing the direction of the flow in the hydraulic circuit. The two sprockets rest on two heavy support beams 1.25 m apart. This allows a maximum length of the test specimen to be 1 m. The bending capacity of the machine is 5300 N-m. Each tube is tested and fitted with a solid rod extension. The contact between the tube and the rollers is free to move along the axial direction during bending. The load transfer to the test specimen is a couple formed by concentrated loads from two of the rollers. The applied bending moment is directly proportional to the tension in the chains. Based on the signal from two load cells, the bending moment is calculated. A detailed explanation of the experimental facility can be found in many papers (Pan and Her [18], Lee et al. [19], Lee et al. [20]).

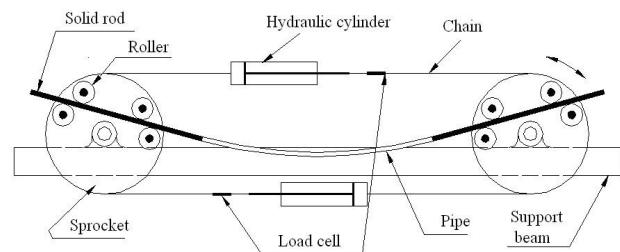


Fig. 2 A schematic drawing of the tube-bending machine

### B. Curvature-Ovalization Measurement Apparatus (COMA)

Fig.3 shows a schematic drawing of the COMA. The COMA is an instrument which can be used to measure the tube curvature and ovalization

of the tube cross-section (Pan et al. [26]). It is a lightweight instrument, which can be mounted close to the tube mid-span. There are three inclinometers in COMA. Two of them are fixed on two holders, which are denoted as side-inclinometers. The holders are fixed on the circular tube before the test begins. The distance between the two side-inclinometers is denoted as  $L_0$ . Let us now consider that the circular tube is subjected to pure bending, as shown in Fig. 4. The angle changes detected by two side-inclinometers are denoted as  $\theta_1$  and  $\theta_2$ . From Fig. 4, the curvature of the tube  $\kappa$  is

$$\kappa = 1 / \rho = (\theta_1 + \theta_2) / L_0 \quad (1)$$

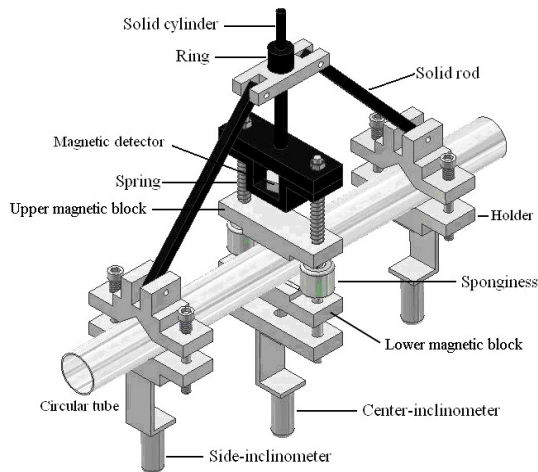


Fig. 3 A schematic drawing of the curvature-ovalization measurement apparatus

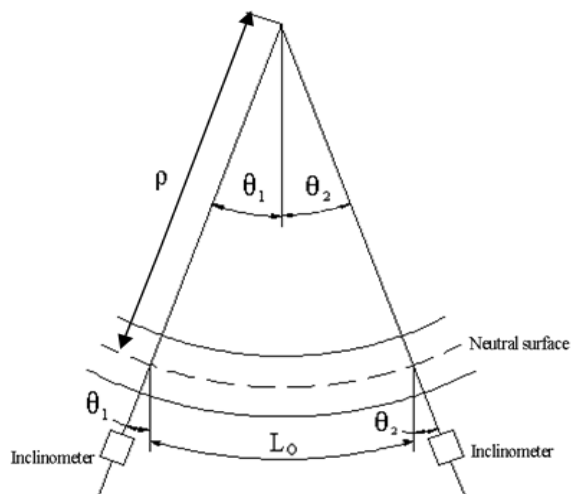


Fig. 4 Longitudinal deformation between two side-inclinometers under pure bending

### C. Material and Specimens

The circular tubes used in this study were made of SUS304 stainless steel. The tubes' chemical composition is Cr (18.36%), Ni (8.43%), Mn (1.81%), Si (0.39%), ..., and a few other trace elements, with the remainder being Fe. The ultimate stress, 0.2% strain offset the yield stress and the percent elongation are 626 MPa, 296 MPa and 35%, respectively. The raw smooth SUS304 stainless steel tube had an outside diameter  $D_o$  of 36.6 mm and wall-thickness  $t$  of 1.5 mm. The raw tubes were machined on the outside surface to obtain the desired local notch depth ( $a$ ) of 0.2, 0.4, 0.6, 0.8 and 1.0 mm. Fig. 5 shows a schematic drawing of the local sharp-notched tube. According to the drill of the machine, the corresponding surface diameters  $b$  were 0.6, 1.2, 1.8, 2.4 and 3.0 mm, respectively.

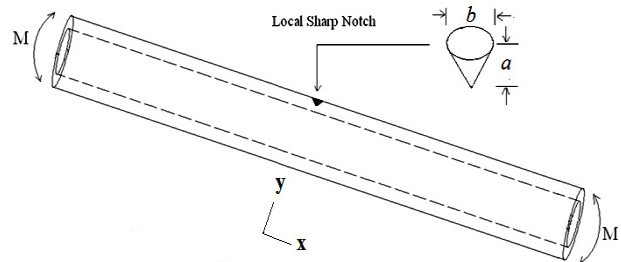


Fig. 5 A schematic drawing of a local sharp-notched tube with a notch depth of  $a$ .

### D. Test Procedures

The bending experiments were performed under curvature-controlled conditions. The curvature rates ( $\dot{\kappa}$ ) for the cyclic bending test were 0.0035, 0.035 and 0.35  $m^{-1}s^{-1}$ . Two load cells installed in the testing facility (Fig. 2) were used to measure the bending moment. The light-weight instrument in Fig. 3 was used to measure the curvature and ovalization. The number of bending cycles required to produce buckling was also recorded.

### III. EXPERIMENTAL RESULTS

#### A. Viscoplastic Response

Fig. 6 shows a typical experimental result of the moment ( $M$ ) - curvature ( $\kappa$ ) curve for a local sharp-notched SUS304 stainless steel tube with  $a = 0.2$  mm submitted to cyclic bending at  $\dot{\kappa} = 0.0035 \text{ m}^{-1}\text{s}^{-1}$ . The tubes were cycled between curvature values of  $\pm 0.3 \text{ m}^{-1}$ . It can be observed that the  $M$ - $\kappa$  response reveals cyclic hardening and became a steady loop after a few bending cycles. Since the sharp notch is small and local, the notch depth has almost no influence on the  $M$ - $\kappa$  curve. Therefore, the  $M$ - $\kappa$  curves for different  $a$  are not shown in this paper.

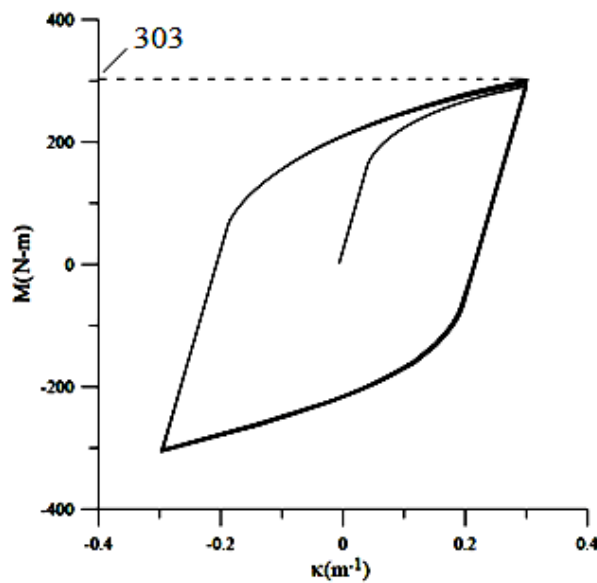


Fig. 6 Experimental moment ( $M$ ) - curvature ( $\kappa$ ) curve for local sharp-notched SUS304 stainless steel tubes with  $a = 0.2$  mm under cyclic bending at  $\dot{\kappa} = 0.0035 \text{ m}^{-1}\text{s}^{-1}$

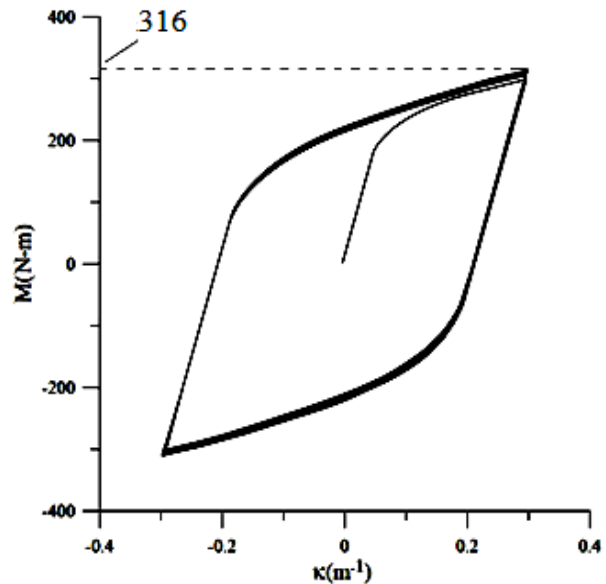


Fig. 7 Experimental moment ( $M$ ) - curvature ( $\kappa$ ) curve for local sharp-notched SUS304 stainless steel tubes with  $a = 0.2$  mm under cyclic bending at  $\dot{\kappa} = 0.035 \text{ m}^{-1}\text{s}^{-1}$

Figs. 7-8 present experimental data of moment ( $M$ ) - curvature ( $\kappa$ ) curves for local sharp-notched SUS304 stainless steel tubes with  $a = 0.2$  mm submitted to cyclic bending at  $\dot{\kappa} = 0.035$  and  $0.35 \text{ m}^{-1}\text{s}^{-1}$ , respectively. It is evident that the  $M$ - $\kappa$  curves demonstrated in Figs. 6-8 are very similar. However, higher  $\dot{\kappa}$  lead to higher maximum moment at  $\kappa = +0.3 \text{ m}^{-1}$ . The maximum moments of 303, 316 and 325 N-m correspond to  $\dot{\kappa} = 0.0035, 0.035$  and  $0.35 \text{ m}^{-1}\text{s}^{-1}$ , respectively. The highest and lowest curvature rates have 100 times difference. But, the maximum moment only increases 7.3%. Due to similar phenomenon, the experiment results of the  $M$ - $\kappa$  response for local sharp-notched SUS304 stainless steel tubes with  $a = 0.4, 0.6, 0.8$  and  $1.0$  mm subjected to cyclic bending at  $\dot{\kappa} = 0.0035, 0.035$  and  $0.35 \text{ m}^{-1}\text{s}^{-1}$  are not shown in this paper.

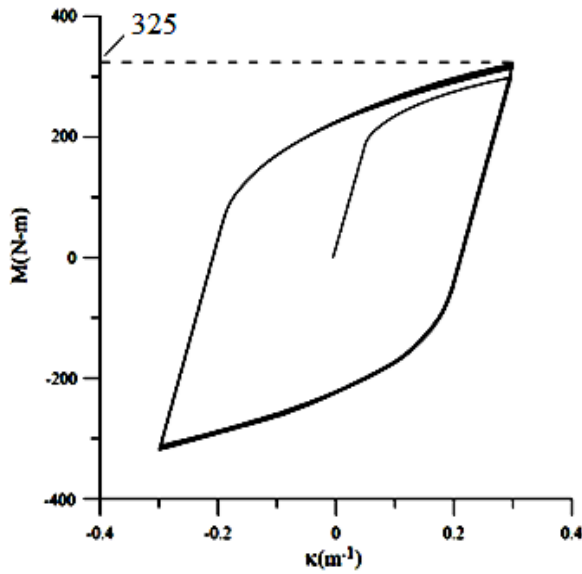


Fig. 8 Experimental moment (M) - curvature ( $\kappa$ ) curve for local sharp-notched SUS304 stainless steel tubes with  $a = 0.2$  mm under cyclic bending at  $\dot{\kappa} = 0.35 \text{ m}^{-1}\text{s}^{-1}$

Figs. 9-13 demonstrate the experimental ovalization ( $\Delta D_o/D_o$ ) - curvature ( $\kappa$ ) curves for local sharp-notched SUS304 stainless steel tubes with  $a = 0.2, 0.4, 0.6, 0.8$  and  $1.0$  mm, respectively, submitted to cyclic bending at  $\dot{\kappa} = 0.035 \text{ m}^{-1}\text{s}^{-1}$ . The ovalization is defined as  $\Delta D_o/D_o$ , where  $\Delta D_o$  is the change in the outside diameter. The maximum ovalizations for the 6<sup>th</sup> cycle are 0.0023, 0.0025, 0.0026, 0.0027 and 0.0028 for  $a = 0.2, 0.4, 0.6, 0.8$  and  $1.0$  mm, respectively. It is observed that the  $\Delta D_o/D_o$ - $\kappa$  curves exhibit a ratcheting trend and increase with the number of bending cycles. A larger  $a$  results in a more asymmetrical look to the  $\Delta D_o/D_o$ - $\kappa$  curve. Moreover, larger  $a$  of notched tubes leads to larger ovalization.

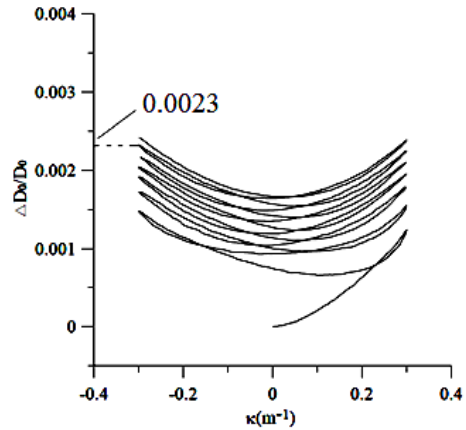


Fig. 9 Experimental ovalization ( $\Delta D_o/D_o$ ) - curvature ( $\kappa$ ) curves for local sharp-notched SUS304 stainless steel tubes with  $a = 0.2$  mm submitted to cyclic bending at  $\dot{\kappa} = 0.035 \text{ m}^{-1}\text{s}^{-1}$

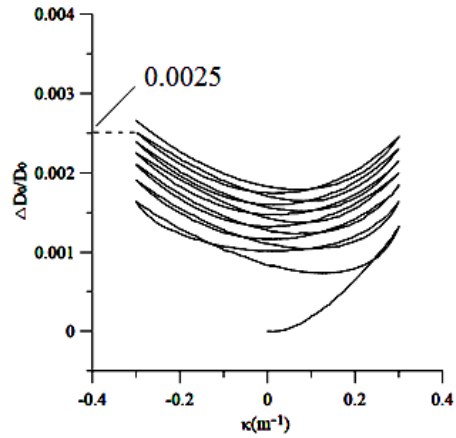


Fig. 10 Experimental ovalization ( $\Delta D_o/D_o$ ) - curvature ( $\kappa$ ) curves for local sharp-notched SUS304 stainless steel tubes with  $a = 0.4$  mm submitted to cyclic bending at  $\dot{\kappa} = 0.035 \text{ m}^{-1}\text{s}^{-1}$

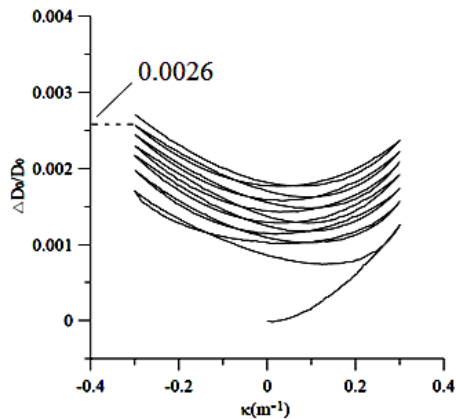


Fig. 11 Experimental ovalization ( $\Delta D_o/D_o$ ) - curvature ( $\kappa$ ) curves for local sharp-notched SUS304 stainless steel tubes with  $a = 0.6$  mm submitted to cyclic bending at  $\dot{\kappa} = 0.035 \text{ m}^{-1}\text{s}^{-1}$

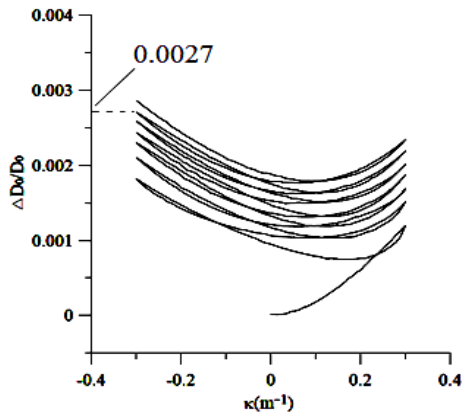


Fig. 12 Experimental ovalization ( $\Delta D_o/D_o$ ) - curvature ( $\kappa$ ) curves for local sharp-notched SUS304 stainless steel tubes with  $a = 0.8$  mm submitted to cyclic bending at  $\dot{\kappa} = 0.0035 \text{ m}^{-1}\text{s}^{-1}$

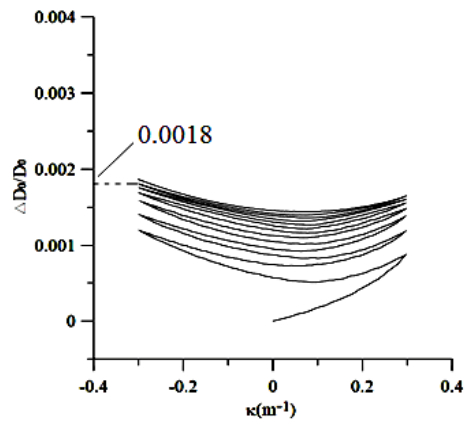


Fig. 14 Experimental ovalization ( $\Delta D_o/D_o$ ) - curvature ( $\kappa$ ) curves for local sharp-notched SUS304 stainless steel tubes with  $a = 0.2$  mm submitted to cyclic bending at  $\dot{\kappa} = 0.0035 \text{ m}^{-1}\text{s}^{-1}$

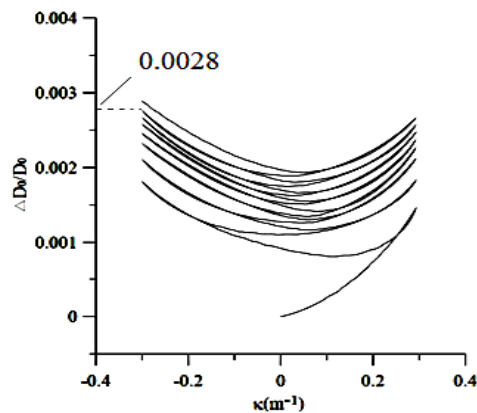


Fig. 13 Experimental ovalization ( $\Delta D_o/D_o$ ) - curvature ( $\kappa$ ) curves for local sharp-notched SUS304 stainless steel tubes with  $a = 1.0$  mm submitted to cyclic bending at  $\dot{\kappa} = 0.0035 \text{ m}^{-1}\text{s}^{-1}$

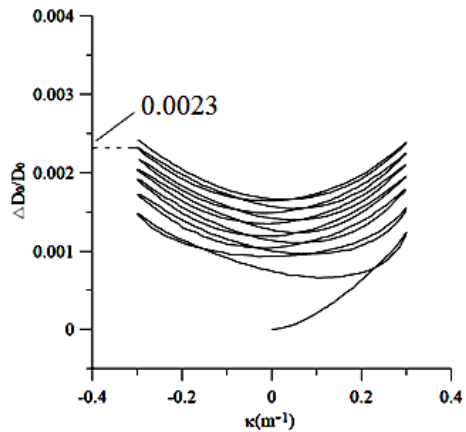


Fig. 15 Experimental ovalization ( $\Delta D_o/D_o$ ) - curvature ( $\kappa$ ) curves for local sharp-notched SUS304 stainless steel tubes with  $a = 0.2$  mm submitted to cyclic bending at  $\dot{\kappa} = 0.035 \text{ m}^{-1}\text{s}^{-1}$

Figs. 14-16 depict the experimental ovalization ( $\Delta D_o/D_o$ ) - curvature ( $\kappa$ ) curves for local sharp-notched SUS304 stainless steel tubes with  $a = 0.2$  mm submitted to cyclic bending at  $\dot{\kappa} = 0.0035$ ,  $0.035$  and  $0.35 \text{ m}^{-1}\text{s}^{-1}$ , respectively. It can be seen that higher  $\dot{\kappa}$  leads to larger ovalization. From Figs. 14, 15 and 16, the maximum ovalizations of  $0.0018$ ,  $0.0023$  and  $0.0032$  at the 6<sup>th</sup> cycle correspond to  $\dot{\kappa} = 0.0035$ ,  $0.035$  and  $0.35 \text{ m}^{-1}\text{s}^{-1}$ , respectively. The highest and lowest  $\dot{\kappa}$  have 100 times difference. However, the maximum ovalization increases 77.8%. It is concluded that the curvature rate has a strong influence on the  $\Delta D_o/D_o$ - $\kappa$  curve. Again, due to similar results, the experimental  $\Delta D_o/D_o$ - $\kappa$  curves for  $a = 0.4$ ,  $0.6$ ,  $0.8$  and  $1.0$  mm at  $\dot{\kappa} = 0.0035$  and  $0.35 \text{ m}^{-1}\text{s}^{-1}$  are not shown.

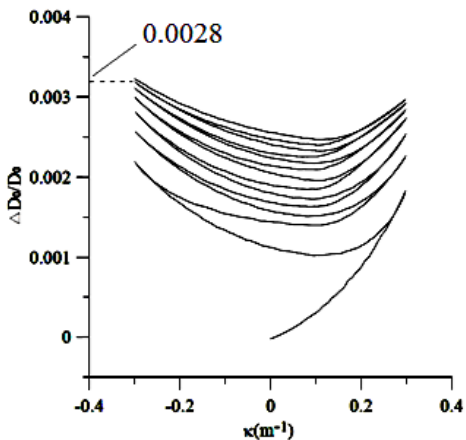


Fig. 16 Experimental ovalization ( $\Delta D_o/D_o$ ) - curvature ( $\kappa$ ) curves for local sharp-notched SUS304 stainless steel tubes with  $a = 0.2$  mm under cyclic bending at  $\dot{\kappa} = 0.35 \text{ m}^{-1}\text{s}^{-1}$

**B. Viscoplastic Buckling**

The experimental data of cyclic curvature ( $\kappa_c$ ) versus the number of bending cycles required to produce buckling ( $N_b$ ) for local sharp-notched SUS304 stainless steel tubes under cyclic bending with  $a = 0.2, 0.4, 0.6, 0.8,$  and  $1.0$  mm at  $\dot{\kappa} = 0.0035, 0.035$  and  $0.35 \text{ m}^{-1}\text{s}^{-1}$ , respectively, are illustrated in Figs. 17-19. For a fixed  $\dot{\kappa}$  and  $\kappa_c$ , a larger  $a$  causes a lower  $N_b$ . For a fixed  $\dot{\kappa}$  and  $a$ , a larger  $\kappa_c$  leads to a lower  $N_b$ . In addition, for a fixed  $\kappa_c$  and  $a$ , a larger  $\dot{\kappa}$  results a lower  $N_b$ .

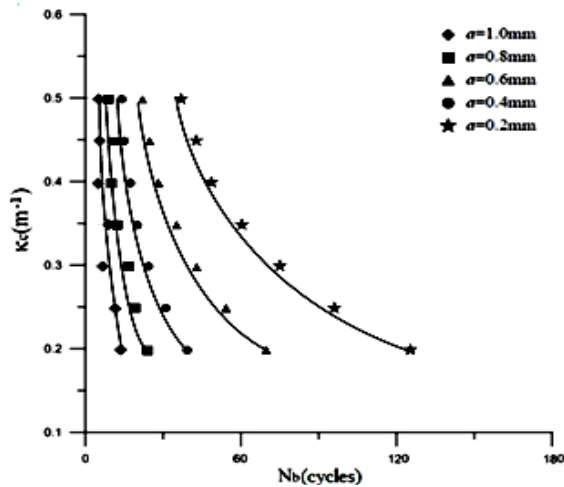


Fig. 17 Experimental controlled curvature ( $\kappa_c$ ) - number of bending cycles required to produce buckling ( $N_b$ ) curves for local sharp-notched SUS304 stainless steel tubes with  $a = 0.2, 0.4, 0.6, 0.8,$  and  $1.0$  mm under cyclic bending at  $\dot{\kappa} = 0.0035 \text{ m}^{-1}\text{s}^{-1}$

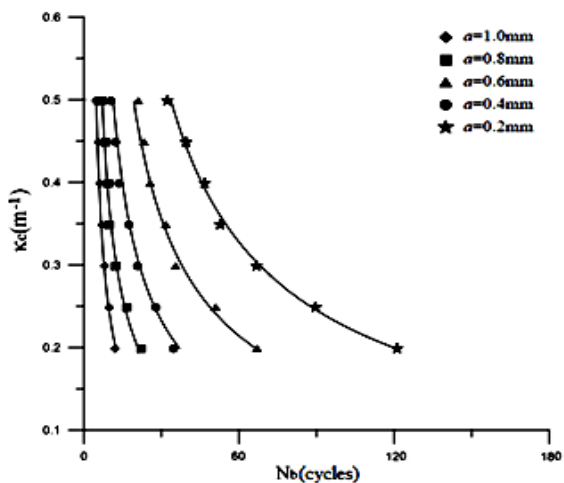


Fig. 18 Experimental controlled curvature ( $\kappa_c$ ) - number of bending cycles required to produce buckling ( $N_b$ ) curves for local sharp-notched SUS304

stainless steel tubes with  $a = 0.2, 0.4, 0.6, 0.8,$  and  $1.0$  mm under cyclic bending at  $\dot{\kappa} = 0.35 \text{ m}^{-1}\text{s}^{-1}$

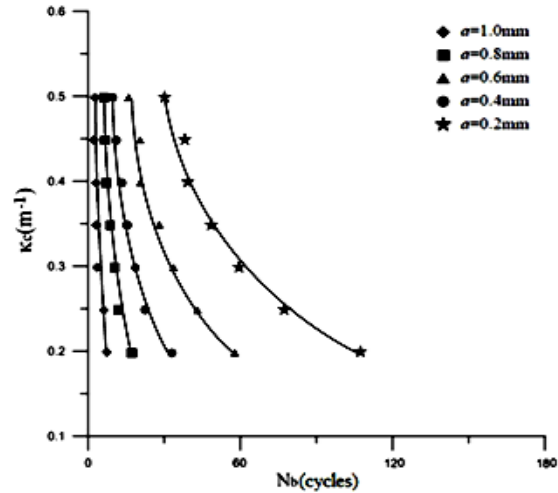


Fig. 19 Experimental controlled curvature ( $\kappa_c$ ) - number of bending cycles required to produce buckling ( $N_b$ ) curves for local sharp-notched SUS304 stainless steel tubes with  $a = 0.2, 0.4, 0.6, 0.8,$  and  $1.0$  mm under cyclic bending at  $\dot{\kappa} = 0.35 \text{ m}^{-1}\text{s}^{-1}$

**IV. CONCLUSIONS**

The response and buckling of local sharp-notched SUS304 stainless steel tubes with different  $a$  subjected to cyclic bending at different  $\dot{\kappa}$  are experimentally discussed in this study. As a result of the experimental results, some important conclusions have been reached and are presented as follows:

- (1) Under symmetrical cyclic bending, the experimental  $M$ - $\kappa$  relationships for local sharp-notched SUS304 stainless steel tubes with any  $a$  at any  $\dot{\kappa}$  exhibits a closed and stable hysteresis loop after a few bending cycles. In addition,  $\kappa$  has a small influence on the  $M$ - $\kappa$  response.
- (2) Under symmetrical cyclic bending, the experimental  $\Delta D_o/D_o$ - $\kappa$  relationships for local sharp-notched SUS304 stainless steel tubes with any  $a$  at any  $\dot{\kappa}$  exhibits an increase and ratcheting with an increase in the number of bending cycles. Larger  $a$  causes more asymmetry and larger ovalization. In addition,  $\dot{\kappa}$  has a profound influence on the  $\Delta D_o/D_o$ - $\kappa$  curves. Higher  $\dot{\kappa}$  leads to larger  $\Delta D_o/D_o$ .
- (3) Under symmetrical cyclic bending, the experimental  $\kappa_c$ - $N_b$  relationships for local sharp-notched SUS304 stainless steel tubes with different  $a$  submitted to cyclic bending at

different  $\kappa$  show that for a fixed  $\kappa$  and  $\kappa_c$ , a larger  $a$  causes a lower  $N_b$ . For a fixed  $\kappa$  and  $a$ , a larger  $\kappa_c$  leads to a lower  $N_b$ . In addition, for a fixed  $\kappa_c$  and  $a$ , a larger  $\kappa$  results a lower  $N_b$ .

## ACKNOWLEDGMENT

The work presented was carried out with the support of the National Science Council under grant MOST 103-2221-E-006-041. Its support is gratefully acknowledged.

## REFERENCES

1. P. K. Shaw, S. Kyriakides, "Inelastic analysis of thin-walled tubes under cyclic bending," *Int. J. Solids Struct.*, vol. 21, no. 11, pp. 1073-1110, 1985.
2. S. Kyriakides and P. K. Shaw, "Inelastic buckling of tubes under cyclic loads," *J. Pres. Ves. Tech.*, vol. 109, no. 2, pp. 169-178, 1987.
3. E. Corona and S. Kyriakides, "An experimental investigation of the degradation and buckling of circular tubes under cyclic bending and external pressure," *Thin-Walled Struct.*, vol. 12, no. 3, pp. 229-263, 1991.
4. E. Corona, S. Kyriakides, "Asymmetric collapse modes of pipes under combined bending and external pressure," *J. Eng. Mech.*, vol. 126, no. 12, pp. 1232-1239, 2000.
5. E. Corona, L. H. Lee and S. Kyriakides, "Yield anisotropic effects on buckling of circular tubes under bending," *Int. J. Solids Struct.*, vol. 43, no. 22-23, pp. 7099-7118, 2006.
6. A. Limam, L. H. Lee and S. Kyriakides, "On the collapse of dented tubes under combined bending and internal pressure," *Int. J. Solids Struct.*, vol. 55, no. 1, pp. 1-12, 2012.
7. N. J. Bechle and S. Kyriakides, "Localization in NiTi tubes under bending," *Int. J. Solids Struct.*, vol. 51, no. 5, pp. 967-980, 2014.
8. W. Yuan and A. Mirmiran, "Buckling analysis of concrete-filled FRP tubes," *Int. J. Struct. Stab. Dyn.*, vol. 1, no. 3, pp. 367-383, 2001.
9. M. Elchalakani, X. L. Zhao and R. H. Grzebieta, "Plastic mechanism analysis of circular tubes under pure bending," *Int. J. Mech. Sci.*, vol. 44, no. 6, pp. 1117-1143, 2002.
10. H. Jiao and X. L. Zhao, "Section slenderness limits of very high strength circular steel tubes in bending," *Thin-Walled Struct.*, vol. 42, no. 9, pp. 1257-1271, 2004.
11. S. Houliara and S. A. Karamanos, "Buckling and post-buckling of long pressurized elastic thin-walled tubes under in-plane bending," *Int. J. Nonlinear Mech.*, vol. 41, no. 4, pp. 491-511, 2006.
12. C. Mathon and A. Liman, "Experimental collapse of thin cylindrical shells submitted to internal pressure and pure bending," *Thin-Walled Struct.*, vol. 44, no. 1, pp. 39-50, 2006.
13. M. Elchalakani and X. L. Zhao, "Concrete-filled cold-formed circular steel tubes subjected to variable amplitude cyclic pure bending," *Eng. Struct.*, vol. 30, no. 2, pp. 287-299, 2008.
14. X. D. Zhi, F. Fan and S. Z. Shen, "Failure mechanism of single-layer cylindrical reticulated shells under earthquake motion," *Int. J. Struct. Stab. Dyn.*, vol. 12, no. 2, pp. 233-249, 2012.
15. L. Guo L., S. Yang and H. Jiao, "Behavior of thin-walled circular hollow section tubes subjected to bending," *Thin-Walled Struct.*, vol. 73, pp. 281-289, 2013.
16. M. Shariati, K. Kolasangiani, G. Norouzi and A. Shahnavaz, "Experimental study of SS316L cantilevered cylindrical shells under cyclic bending load," *Thin-Walled Struct.*, vol. 82, pp. 124-131, 2014.
17. M. Elchalakani, A. Karrech, M. F. Hassanein and B. Yang, "Plastic and yield slenderness limits for circular concrete filled tubes subjected to static pure bending," *Thin-Walled Struct.*, vol. 109, pp. 50-64, 2016.
18. W. F. Pan and Y. S. Her, "Viscoplastic collapse of thin-walled tubes under cyclic bending," *J. Eng. Mat. Tech.*, vol. 120, no. 4, pp. 287-290, 1998.
19. K. L. Lee, W. F. Pan and J. N. Kuo, "The influence of the diameter-to-thickness ratio on the stability of circular tubes under cyclic bending," *Int. J. Solids Struct.*, vol. 38, no. 14, pp. 2401-2413, 2001.
20. K. L. Lee, R. F. Shie and K. H. Chang, "Experimental and theoretical investigation of the response and collapse of 316L stainless steel tubes subjected to cyclic bending," *JSME Int. J., Ser. A*, vol. 48, no. 3, pp. 155-162, 2005.
21. K. H. Chang and W. F. Pan, "Buckling life estimation of circular tubes under cyclic bending," *Int. J. Solids Struct.*, vol. 46, no. 2, pp. 254-270, 2009.
22. K. L. Lee, C. Y. Hung and W. F. Pan, "Variation of ovalization for sharp-notched circular tubes under cyclic bending," *J. Mech.*, vol. 26, no. 3, pp. 403-411, 2010.

23. K. L. Lee, "Mechanical behaviour and buckling failure of sharp-notched circular tubes under cyclic bending," *Struct. Eng. Mech.*, vol. 34, no.3, pp. 367-376, 2010.
24. K. L. Lee, C. M. Hsu and W. F. Pan, "Viscoplastic collapse of sharp-notched circular tubes under cyclic bending," *Acta Mech. Solida Sinica*, vol. 26, no.6, pp. 629-641, 2013.
25. K. L. Lee, C. H. Meng and W. F. Pan, "The influence of notch depth on the response of local sharp-notched circular tubes under cyclic bending," *J. Appl. Math. Phy.*, vol. 2, no. 6, pp. 335-341, 2014.
26. W. F. Pan, T. R. Wang and C. M. Hsu, "A curvature-ovalization measurement apparatus for circular tubes under cyclic bending," *Exp. Mech.*, vol. 38, no.2, pp. 99-102, 1998.